

May 2014

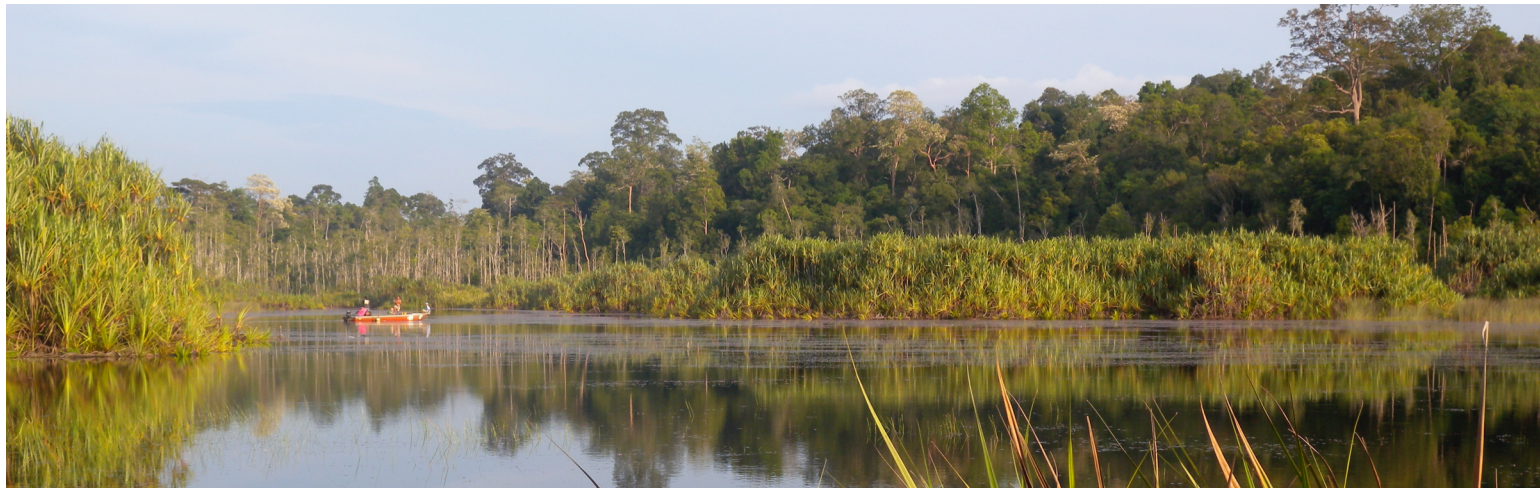


- General Lake Model

Model Overview and User Information

v 1.4.0 - DRAFT May 2014

M.R. Hipsey, L.C. Bruce & D.P. Hamilton



THE UNIVERSITY OF
WESTERN AUSTRALIA



THE UNIVERSITY OF
WAIKATO
Tē Whare Hinanga o Waikato



Summary

The General Lake Model (GLM) is an open-access model developed for simulating lake dynamics. It simulates vertical stratification and mixing and accounts for the effect of inflows/outflows, surface heating and cooling, and it can be extended to include the effect of ice cover. GLM has been designed to be an open-source community model developed in collaboration with members of *Global Lake Ecological Observatory Network* (GLEON) to integrate with lake sensor data.

It is suited to environmental modelling studies where simulation of lakes or reservoirs is required. The one-dimensional (1D) basis of the model means it is suited to seasonal and decadal scale investigations of water quality but it can also be used in comparisons of simulation output against high-frequency sensor data. Sites that may be simulated with the model include deep and shallow lakes, drinking water, hydropower or irrigation reservoirs, mining pit lakes, wastewater ponds and urban wetlands. The model couples with the *Aquatic EcoDynamics* library (AED) for integrated simulations of lake and reservoir water quality and ecosystem health.

This manual summarises the scientific basis and numerical implementation of the model algorithms including the sub-models related to surface heat exchange and ice-cover dynamics, vertical mixing and the inflow/outflow dynamics. A summary of typical parameter values for lakes and reservoirs collated from a range of sources is included. The final section provides an overview of setting up and running the model. Further information for analysis of model outputs and undertaking sensitivity and uncertainty assessments with the model is also provided.

Acknowledgements

GLM has been developed by the Aquatic EcoDynamics Research Group team at UWA (<http://aed.see.uwa.edu.au>) in collaboration with the Lake Ecosystem Restoration research group at the University of Waikato (<http://www.lernz.com>). Funding for the initial development of the model was from the U.S. NSF Cyber-enabled Discovery and Innovation (CDI) grant awarded to Prof. Paul Hanson (lead investigator) and colleagues from 2009-2014. In addition to the named authors we acknowledge the software engineering of the model undertaken by Casper Boon at UWA. We acknowledge also numerous members of the GLEON ecosystem modelling working group and the associated multi-lake comparison project (MLCP). As a result of this work we have undertaken extensive review of model performance on preliminary versions and provided extensive feedback on model features and operation. Whilst GLM is a new code, it is based on the large body of historical research and publications produced by the Centre for Water Research at the University of Western Australia, which we acknowledge for the inspiration and guidance on the approach that has been adopted herein. We also acknowledge the MCMC code by Marko Laine that has been integrated with this GLM version model sensitivity and uncertainty assessment, (accessed from <http://helios.fmi.fi/~lainema/mcmc/>). Provision of the environmental symbols used for the GLM scientific diagrams are courtesy of the Integration and Application Network, University of Maryland Center for Environmental Science.

Citing this manual:

Hipsey, M.R., Bruce, L.C., Hamilton, D.P., 2014. GLM - General Lake Model: Model overview and user information. AED Report #26, The University of Western Australia, Perth, Australia. 22pp.

Copyright © 2014. The University of Western Australia.

ISBN: 978-1-74052-303-5



Contents

SUMMARY	1
CONTENTS	3
THE GENERAL LAKE MODEL (GLM)	4
OVERVIEW	4
MODEL DESCRIPTION	5
Layer structure	5
Energy budget	6
Surface mass fluxes	7
Snow & ice model	7
Vertical mixing	9
Inflows and outflows	10
MODEL SUITABILITY & DATA REQUIREMENTS	12
SETUP & OPERATION	14
OVERVIEW	14
INPUT FILES	14
Physical model configuration: <code>glm.nml</code>	14
Meteorology: <code>met.csv</code>	15
Inflows: <code>inflows.csv</code>	16
Outflows: <code>outflows.csv</code>	16
RUNNING THE MODEL	18
OUTPUTS AND POST-PROCESSING	18
Live output plotting: <code>plots.nml</code>	18
Plotting in EXCEL	19
Plotting in R	19
Plotting in MATLAB	19
Plotting with PyNCview	Error! Bookmark not defined.
MODEL VALIDATION & PARAMETER OPTIMISATION	19
Running the LakeAnalyzer validation	19
Running the MCMC parameter estimation	21
EXAMPLES & SUPPORT	22
DOWNLOADS & FURTHER SUPPORT	22
EXAMPLE APPLICATIONS	22
REFERENCES	23



The General Lake Model (GLM)

Overview

The **General Lake Model** (GLM) is a one-dimensional hydrodynamic model for simulating the water balance and vertical stratification of lakes and other standing (lentic) water bodies. GLM computes vertical profiles of temperature, salinity and density by accounting for the effect of inflows and outflows on the water balance, in addition to surface heating and cooling, and vertical mixing (Figure 1). The model also includes the effects of ice cover formation and subsequent melting on the heating and mixing processes within the lake.

Since the model is one-dimensional it assumes no horizontal variability within the domain and users must therefore ensure their application of the model is suited to this assumption. For deep, stratified, systems, the model is ideally suited to long-term investigations ranging from months to decades, and for coupling with biogeochemical models to explore the role that stratification and vertical mixing play on lake ecosystem dynamics. However, the model can also be used, with some caution and checks, for shallow lakes, ponds or wetlands where the water column is relatively well mixed.

The model was initially built as a project within the **Global Lake Ecological Observatory Network** (GLEON) to provide a computationally efficient lake modelling platform to be used for integration with lake observatory systems and for training lake scientists. The model couples with the **Framework for Aquatic Biogeochemical Models** (FABM), and in particular is designed to operate with the **Aquatic EcoDynamic** modules (Hipsey et al., 2014) included within FABM (termed **FABM-AED**). Since its original development, the model has also been used successfully for simulating reservoirs, mining pit lakes and wetlands. The model is available freely and distributed as open-source under the GNU GPL license.

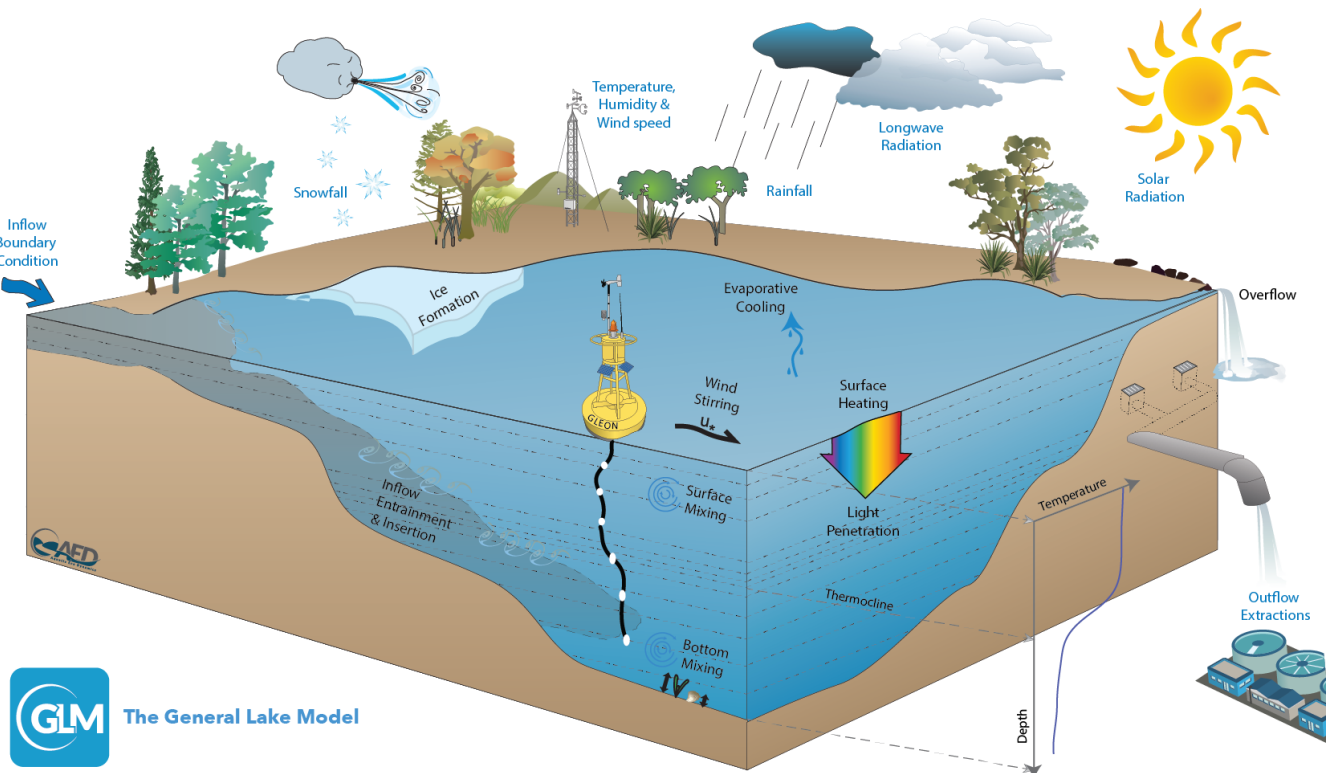


Figure 1: Schematic of a GLM simulation domain, input information (blue text) and key simulated processes (black text).

Model Description

GLM incorporates a series of vertical layers that are used to describe the water column properties. The model adopts a flexible Lagrangian structure originally introduced for the model DYRESM by Imberger et al. (1978) and Imberger & Patterson (1981). Numerous model variations have since been introduced to further extend this conceptual approach through applications to a variety of lake and reservoir environments (e.g., Hocking & Patterson, 1991; Hamilton & Schladow 1997; McCord & Schladow, 1998; Gal et al., 2003; Yeates et al., 2004). The Lagrangian design assumes each layer is a 'control volume' that can change thickness by contracting and expanding in response to inflows, outflows, mixing with adjacent layers, and surface mass fluxes. Layers each have a unique density computed based on the local salinity and temperature and when sufficient energy becomes available to overcome density differences between the adjacent layers, they will merge thus accounting for the process of mixing. For deeper systems, a stable vertical density gradient will form in response to periods of high solar radiation creating warm, less-dense conditions near the surface with cooler conditions deeper in the water column separated by a thermocline region (metalimnion). Layer thicknesses are adjusted throughout the water column by the model in order to sufficiently resolve the vertical density gradient with fine resolution occurring in the thermocline and thicker cells where mixing is occurring (as depicted schematically in Figure 1). Unlike the fixed grid (Eulerian) design of most lake and ocean models, where mixing algorithms are typically based on resolving vertical velocities, it has been reported that numerical diffusion of the thermocline in this approach is limited, making it particularly suited to long-term investigations, and requiring limited site-specific calibration (Patterson et al., 1984; Hamilton & Schladow, 1997).

Although GLM is a new model code written in C, the core layer structure and mixing algorithms have been based on equations summarised in Hamilton and Schladow (1997), thereby making it similar to these previously reported models. Beyond this functionality, the model features numerous customisations and extensions in order to make it a fast and easy to use package suitable for a wide range of contemporary applications.

Layer structure

The model is composed of a series of layers numbered from the lake bottom to the surface. The number of layers, $N_{LEV}(t)$, is adjusted throughout the simulation to maintain the assumption that each layer must have homogenous properties across the layer. Initially, the layers are assumed to be of equal thickness, and the initial number of layers, $N_{LEV}(t = 0)$, depends on the user-defined minimum (h_{min}) and maximum (h_{max}) layer thickness limits that are set, and the lake depth (both defined in `glm.nml`, see model setup section). As the model simulation progresses, density changes due to surface heating, vertical mixing, and inflows and outflows lead to dynamic changes in the layer structure as layers expand or contract. The model includes routines to enforce the layer limits, maintaining the optimal thickness of layers required to resolve the vertical density gradient.

The layer volumes are determined by interpolating layer area off the user-specified hypsographic curve for the lake basin, such that $A_i = f(h_i)$, where i is the layer number. The user provides N_{BSN} depth points with basin area to define the hypsographic curve. Layers are generally at a relatively coarse resolution relative to the simulated layers, and the model can either i) accept prescribed volume values at each, or ii) compute the volumes assuming a simple interpolation. In the latter case, the first layer, V_1 , is computed assuming a conical shape, and above that each point as:

$$V_b = V_{b-1} + [A_{b-1} + 0.5(A_b - A_{b-1})](h_b - h_{b-1})$$

where $1 < b \leq N_{BSN}$. Using the raw hypsographic data, a refined depth-area-volume relationship is calculated during the simulation using finer depth increments (e.g., ~ 0.1 m), giving N_{MORPH} levels that are used for subsequent calculations. The area and volume at the depth of each increment, h_z is interpolated from the supplied information as:

$$V_z = V_{b-1} \left(\frac{h_z}{h_{b-1}} \right)^{\alpha_b} \quad \text{and} \quad A_z = A_{b-1} \left(\frac{h_z}{h_{b-1}} \right)^{\beta_b}$$

where V_z and A_z are the volume and area at each of the refined elevations of the refined depth vector, and V_z in these expressions refers to the nearest b level below h_z such that $h_{b-1} < h_z$. Note the interpolation coefficients are computed as:



$$\alpha_b = \left[\frac{\log_{10}\left(\frac{V_{b+1}}{V_b}\right)}{\log_{10}\left(\frac{h_{b+1}}{h_b}\right)} \right] \quad \text{and} \quad \beta_b = \left[\frac{\log_{10}\left(\frac{A_{b+1}}{A_b}\right)}{\log_{10}\left(\frac{h_{b+1}}{h_b}\right)} \right]$$

The density in each layer is computed based on the temperature, T , and salinity, S , at any given time according to the UNESCO (1981) equation of state:

$$\rho_i = \rho(T_i, S_i)$$

Energy budget

A balance of shortwave radiation fluxes, net long wave radiation fluxes, sensible heat and latent heat of evaporative fluxes determine the net cooling and heating for GLM. The model accounts for the surface fluxes of sensible heat and latent heat using commonly adopted bulk aerodynamic formulae.

For sensible heat:

$$\phi_H = -\rho_a c_p C_H U_x (T_a - T_s)$$

where c_p is the specific heat capacity of water, C_H is the bulk aerodynamic coefficient for sensible heat transfer ($=1.3 \times 10^{-3}$), T_a the air temperature ($^{\circ}\text{C}$) and T_s the temperature of the surface layer ($^{\circ}\text{C}$).

For latent heat:

$$\phi_E = -\rho_a C_E U_x (e_a[T_a] - e_s[T_s])$$

where C_E is the bulk aerodynamic coefficient for latent heat transfer, e_a the air vapour pressure and e_s the saturation vapour pressure at the surface layer temperature (hPa). The vapour pressure can be calculated by the following formulae:

$$e_s[T_s] = \exp \left[2.303 \left(7.5 \frac{T_s}{T_s + 273.15} \right) + 0.7858 \right] \quad \text{Option 1}$$

$$e_s[T_s] = 10^{\left(9.28603523 \frac{2322.37885 T_s}{T_s + 273.15} \right)} \quad \text{Option 2}$$

$$e_a[T_a] = \frac{RH}{100} e_s[T_a]$$

Energy fluxes to account for shortwave and longwave radiation are also included in the model. Shortwave radiation is able to penetrate according to the Beer-Lambert Law, and longwave radiation can either be specified as net flux or incoming flux. The incoming flux may be specified directly or calculated by the model based on the cloud cover fraction and air temperature.

Shortwave radiation is calculated as:

$$\phi_{SW}(z) = (1 - \alpha_{SW}) \hat{\phi}_{SW} \exp[-K_d z]$$

$$\alpha_{SW} = \begin{cases} 0.08 + 0.02 \sin \left[\frac{2\pi}{365} d - \frac{\pi}{2} \right] & : \text{northern hemisphere} \\ 0.08 & : \text{equator} \\ 0.08 - 0.02 \sin \left[\frac{2\pi}{365} d - \frac{\pi}{2} \right] & : \text{southern hemisphere} \end{cases}$$

Where $\phi_{SW}(z)$ is the short-wave radiation at depth z (m), α_{SW} is used to account for the effect of albedo on the penetration of ϕ_{SW} and d is the day of the year

Long wave radiation is calculated as:

$$\phi_{LW_{in}} = \sigma [T_a + 273.15]^4 \times (1 + c_1 C) \times (1 - c_2 \exp[-c_3 T_a^2]) \quad (6)$$

$$\phi_{LW_{out}} = \varepsilon_w \sigma [T_s + 273.15]^4$$

$$\phi_{LW_{net}} = \phi_{LW_{in}} - \phi_{LW_{out}}$$

where σ is the Stefan-Boltzman constant, C the cloud cover fraction (0-1), ε_w the emissivity of the water surface and constants, $c_1 = 0.275$; $c_2 = 0.261$; $c_3 = 0.000777 \times 10^{-4}$.



Surface mass fluxes

The model accounts for surface mass fluxes of evaporation, rainfall and snowfall (m day^{-1}):

$$\frac{dh_s}{dt} = \lambda\phi_E + R + S$$

where h_s is the height of the surface layer (m), t time step (s), λ latent heat of evaporation. Note that this equation does not include changes to h_s as a result of mixing dynamics or ice formation/melt as described in the following sections.

Snow and ice model

The algorithms for GLM ice and snow dynamics are based on previous ice modelling studies (Patterson and Hamblin, 1988; Gu and Stefan, 1993; Rogers et al., 1995; Vavrus et al., 1996). To solve the heat transfer equation, the ice model uses a quasi-steady assumption that the time scale for heat conduction through the ice is short relative to the time scale of meteorological forcing (Patterson and Hamblin, 1988; Rogers et al., 1995).

The steady-state conduction equations, which allocate shortwave radiation into two components, a visible ($A_1=70\%$) and an infra-red ($A_2=30\%$) spectral band, which are used with a three-component ice model that includes blue ice (or black ice), snow ice (or white ice) and snow (see Eq. 1 and Fig. 5 of Rogers et al., 1995). Snow ice is generated in response to flooding, when the mass of snow that can be supported by the ice cover is exceeded (see Eq. 13 of Rogers et al., 1995). By assigning appropriate boundary conditions to the interfaces and solving the quasi-steady state of heat transfer numerically, one can determine the upward conductive heat flux between the ice or snow cover and the atmosphere, Φ_0 . The estimation of Φ_0 involves the application of an empirical equation (Ashton, 1986) to estimate snow conductivity (K_s) from its density, where the density of snow is determined as outlined in Figure 1.

At the ice (or snow) surface, a heat flux balance is employed to provide the condition for surface melting,

$$\begin{aligned}\phi_0(T_0) + \phi_{net}(T_0) &= 0 & T_0 < T_m \\ &= -\rho L \frac{dh_i}{dt} & T_0 = T_m\end{aligned}$$

where L is the latent heat of fusion (see physical constants, Table 2), h_i is the height of the upper snow or ice layer, t is time, ρ is the density of the snow or ice, determined from the surface medium properties, T_0 is the temperature at the solid surface, T_m is the melt-water temperature (0°C) and $\phi_{net}(T_0)$ is the net incoming heat flux, at the solid surface:

$$\phi_{net}(T_0) = \phi_{LWin} - \phi_{LWout}(T_0) + \phi_H(T_0) + \phi_E(T_0) + \phi_R(T_0)$$

where ϕ_{LWin} and ϕ_{LWout} are incoming and outgoing longwave radiation, ϕ_H and ϕ_E are sensible and evaporative heat fluxes between the solid boundary and the atmosphere, and ϕ_R is the heat flux due to rainfall. These heat fluxes are calculated as above with modification for determination of vapor pressure over ice or snow (Gill, 1982) and the addition of the rainfall heat flux (Rogers et al., 1995). T_0 is determined using a bilinear iteration until surface heat fluxes are balanced (i.e. $\phi_0(T_0) = -\phi_{net}(T_0)$) and T_0 is stable ($\pm 0.001^\circ\text{C}$). In the presence of ice (or snow) cover, surface temperature $T_0 > T_m$ indicates that energy is available for melting. The amount of energy for melting is calculated by setting $T_0 = T_m$ to determine the reduced thickness of snow or ice (as shown in Eq. 1).

Accretion or ablation of ice is determined through the heat flux at the ice-water interface, q_f . Solving for heat conduction through ice yields:

$$q_f = q_0 - A_1 I_0 \{1 - \exp(-\lambda_{s1} h_s - \lambda_{e1} h_e - \lambda_{l1} h_l)\} - A_2 I_0 \{1 - \exp(-\lambda_{s2} h_s - \lambda_{e2} h_e - \lambda_{l2} h_l)\} - Q_{si} h_s,$$

where I_0 is the shortwave radiation penetrating the surface, λ and h are the light attenuation coefficient and thickness of the ice and snow components designated with subscripts s , i and e for snow, blue ice and snow ice respectively, and Q_{si} is a volumetric heat flux for formation of snow ice, which is given in Eq. 14 of Rogers et al. (1995). Ice and snow light attenuation coefficients are fixed to the same values as those given by Rogers et al. (1995). Reflection of shortwave radiation from the ice or snow surface is a function of surface temperature and ice and snow thickness (see Table 2, Vavrus et al., 1996). Values of albedo derived from these functions vary from 0.08 to 0.6 for ice and from 0.08 to 0.7 for snow.



The imbalance between q_f and the heat flux from the water to the ice, q_w , gives the rate of change of ice thickness at the interface with water:

$$\frac{dh_i}{dt} = \frac{q_f - q_w}{\rho_i L},$$

where ρ_i is the density of blue ice and q_w is given by a finite difference approximation of the conductive heat flux from water to ice:

$$q_w = -K_w \frac{\Delta T}{\Delta z},$$

where K_w is molecular conductivity and ΔT is the temperature difference between the surface water and the bottom of the ice, which occurs across an assigned depth Δz . A value for Δz of 0.5 m is usual, based on the reasoning given in Rogers et al. (1995) and the typical vertical resolution of a model simulation (0.125 – 1.5 m). Note that a wide variation in techniques and values is used to determine the basal heat flux immediately beneath the ice pack (e.g., Harvey, 1990).

Figure 1 shows the overall decision tree to update ice cover, snow cover and water depth. The ice cover equations are applied when water temperature first drops below 0 °C. The ice thickness is set to its minimum value of 0.05 m, which is suggested by Patterson and Hamblin (1988) and Vavrus et al. (1996). The need for a minimum ice thickness relates primarily to horizontal variability of ice cover during the formation and closure periods. The ice cover equations are discontinued and open water conditions are restored in the model when the thermodynamic balance first produces ice thickness < 0.05 m. The effects of snowfall, rainfall, and compaction of snow are described through appropriate choice of one of several options, depending on the air temperature and whether ice or snow is the upper boundary (Figure 1).

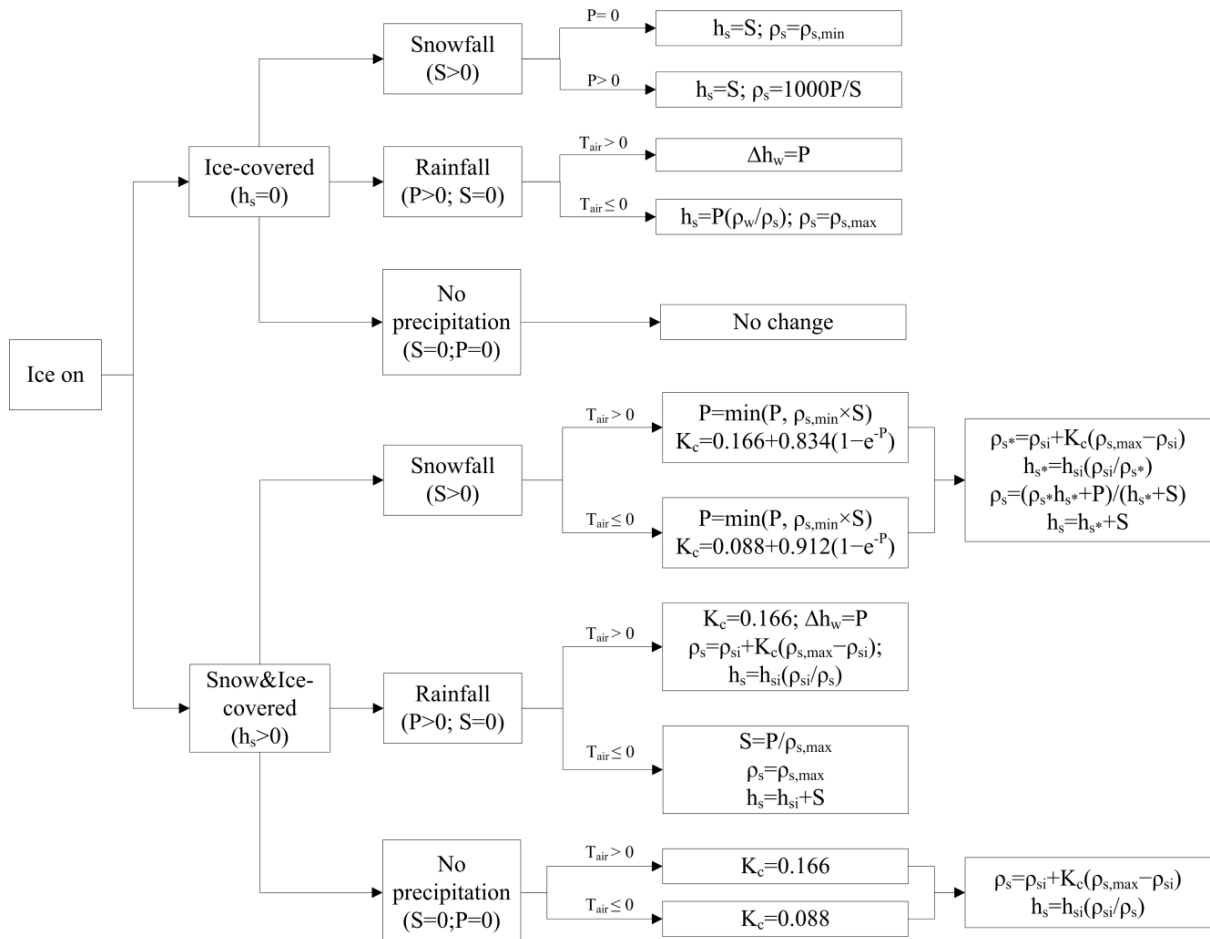


Figure 1: Decision tree to update ice cover, snow cover and water depth according to snow compaction, rainfall (P) and snowfall (S) on each day, and depth of snow cover (h_{s1}) and snow density (ρ_{s1}) for the previous day. Refer to Table 1 for definitions of other variables.

Density of fresh snowfall is determined as the ratio of measured snowfall height to water-equivalent height, with any values exceeding the assigned maximum snow density ($\rho_{max} = 300 \text{ kg m}^{-3}$) truncated to the upper limit. The snow compaction model is based on the exponential decay formula of McKay (1968), with selection of snow compaction parameters based on air temperature (Rogers et al., 1995) as well as on rainfall or snowfall. The approach of snow compaction used by Rogers et al. (1995) is to set the residual snow density to its maximum value when there is fresh snowfall. This method is found to produce increases in snow density that are too rapid when there is only light snowfall. As a result a gradual approach to increasing snow compaction is adopted.

Vertical mixing

Surface Mixed Layer: The GLM works on the premise that the balance between the available energy, E_{TKE} , and the required energy to undergo mixing, E_{PE} , provides for the surface mixed layer (SML) deepening rate dz_{SML}/dt . The model calculates the available kinetic energy due to contributions from wind stirring, shear production between layers, convective overturn, and Kelvin-Helmholtz billowing, which combined are summarised according to:

$$E_{TKE} = \underbrace{0.5C_K(w_*^2) \Delta t}_{\text{convective overturn}} + \underbrace{0.5C_W(\psi^3 u_*^3) \Delta t}_{\text{wind stirring}} + \underbrace{0.5 C_S \left[u_b^2 + \frac{u_b^2 d\xi}{6 dh} + \frac{u_b \xi}{3} \frac{du_b}{dh} \right] h_{s-1}}_{\substack{\text{shear production} \\ \text{K-H production}}}$$

where u_* and w_* refer to the velocity scales in the horizontal and vertical respectively. The energy required to lift up water at the bottom of the mixed layer, denoted here as layer $i - 1$, with thickness Δz_{i-1} , and accelerate it to the SML velocity is required for mixing to occur. This also accounts for energy consumption associated with K-H production and expressed as, E_{PE} :

$$E_{PE} = \left[\underbrace{0.5C_T(w_*^3 + \psi^3 u_*^3)^{2/3}}_{\text{acceleration}} + \underbrace{\frac{\Delta \rho g h_{mix}}{\rho_o}}_{\text{lifting}} + \underbrace{\frac{g \xi^2}{24 \rho_o} \frac{d(\Delta \rho)}{dh} + \frac{g \xi \Delta \rho}{12 \rho_o} \frac{d \xi}{dh}}_{\text{K-H consumption}} \right] h_{s-1}$$

For these equations, the length scale of the K-H billows is summarised as:

$$\xi = KH \frac{\rho_o u_b^2}{g \Delta \rho}$$

where KH is a measure of the mixing efficiency of Kelvin-Helmholtz turbulent billows, and the velocity of the lower layer is approximated from:

$$u_b = \frac{u_*^2 t}{z_{mix}} + u_o$$

The model first calculates these energy arguments and then loops through layers from the top to the bottom until there is insufficient energy available to lift the layer considered up to the next i^{th} layer.

Deep Mixing: Mixing below the SML, in deeper stratified regions of the water column, is modelled using a characteristic diffusivity, $K_z = K_e + K_m$, where K_m is the fixed molecular diffusivity of scalars. The model adopted in GLM is based on the derivation by Weinstock (1981) that is described as being suitable for regions displaying weak or strong stratification, whereby diffusivity increases with dissipation and decreased with heightened stratification:

$$K_z = \frac{\alpha_{TKE} \varepsilon_{TKE}}{N^2 + 0.6 k_{TKE}^2 u_*^2}$$

where α_{TKE} is the mixing efficiency of hypolimnetic TKE (~0.8 in Weinstock, 1981) and k_{TKE} is the turbulence wavenumber:

$$k_{TKE} = \frac{12.4 A_{top}}{\tilde{V} \Delta z_{top} 10^3}$$

and

$$u_* = \sqrt{1.612 \times 10^{-6} U_x^2}$$



The term N^2 is the Brunt–Väisälä (buoyancy) frequency:

$$N^2 = \frac{g\Delta\rho}{\rho\Delta z} \approx \left[\frac{g(\rho_{i+2} - \rho_{i-2})}{\rho_{ref}(h_{i+2} - h_{i-2})} \right]$$

Estimating the turbulent dissipation rate is complex but GLM adopts the approach described in Fischer et al. (1980) where a “net dissipation” is approximated by assuming dissipation is in equilibrium with energy inputs from external drivers:

$$\varepsilon_{TKE} \approx \overline{\varepsilon_{TKE}} = E_{WIND} + E_{INFLOW}$$

which is expanded and calculated per unit volume as:

$$\varepsilon_{TKE} = \underbrace{\frac{1}{(\tilde{V}\bar{\rho})10^3} \frac{m C_D \rho_a f_S U_x^3 A_l}{10^6}}_{\text{rate of working by wind}} + \underbrace{\frac{1}{(V_{mix}\bar{\rho})10^3} \sum_i^{N_{INF}} g \Delta\rho_i Q_i (h_{top} - h_i)}_{\text{rate of working done by inflows}}$$

The diffusivity is calculated according to Eq X, but since the dissipation is assumed to concentrate close to the level of strongest stratification, the “mean” diffusivity is modified to decay exponentially with distance from the thermocline:

$$K_{z_l} = \begin{cases} 0 & h_l \geq (h_{top} - z_{mix}) \\ K_z \exp \left[\frac{-(h_{top} - z_{mix} - h_l)^2}{\sigma} \right] & h_l < (h_{top} - z_{mix}) \end{cases}$$

where σ is the variance of the N^2 distribution below h_{mix} and scales the depth over which mixing decays.

Once the diffusivity is approximated, the diffusion of any scalar, C , between two layers is numerically accounted for by the following mass transfer expressions:

$$C_{i+1} = \bar{C} + \frac{\exp(-f)\Delta z_i \Delta C}{(\Delta z_{i+1} + \Delta z_i)}$$

$$C_i = \bar{C} - \frac{\exp(-f)\Delta z_{i+1} \Delta C}{(\Delta z_{i+1} + \Delta z_i)}$$

where \bar{C} is the weighted mean concentration of C for the two layers, and ΔC is the concentration difference between them. f is related to the diffusivity according to:

$$f = \frac{K_{z_{i+1}} + K_{z_i}}{(\Delta z_{i+1} + \Delta z_i)^2} \Delta t$$

The above diffusion algorithm is run once up the water column and once down the water column as a simple explicit method for capturing diffusion to both the upper and lower layers.

Inflows and outflows

Any number of inflows to the domain can be specified and these are applied at the end of the sub-daily loop, i.e. once a day. Depending on the density of the river water, the inflow will form a positive or negatively buoyant intrusion. As the inflow crosses layers it will entrain water until it reaches a level of neutral buoyancy. At its point of neutral buoyancy it is then assumed to insert as a new layer of thickness dependent on the inflow volume at that time (including additions from entrainment); it may then amalgamate with adjacent layers depending on numerical criteria within the model.

The model operates by estimating the increase in inflow thickness due to entrainment by:

$$h_i = 1.2E dx + h_{i-1}$$

where h_i is the inflow thickness, E is the entrainment rate and dx is the distance travelled by the inflowing water, calculated from the flow rate and inflow thickness. For the initial calculation:

$$h_0 = \left(2Q_i^2 \frac{Ri}{g'} \tan^2 \beta \right)^{0.2}$$

where Q is the flow rate provided as a boundary condition, Ri is the Richardson number, g' is reduced gravity and beta is the slope of the inflow at the point where it meets the water body. The flow is estimated to increase according to:

$$Q_i = Q_{i-1} \left[\left(\frac{h_i}{h_{i-1}} \right)^{5/3} - 1 \right]$$

and E is calculated from either:

$$E = \frac{3}{4} \left[\frac{5 \tan \Phi}{F^2} - \frac{5C_D}{\sin \beta} \right] \frac{F^2}{(3F^2 + 2)}$$

or:

$$E = 1.6 \frac{C_D^{1.5}}{Ri}$$

where C_D is the user specified drag coefficient for the inflow and Ri of the inflow is estimated from:

$$Ri = \frac{C_D \left(1 + 0.21C_D \sin \left[\frac{\beta\pi}{180} \right] \right)}{\sin \left[\frac{\beta\pi}{180} \right] \sin \left[\frac{\Phi\pi}{180} \right] / \cos \left[\frac{\Phi\pi}{180} \right]}$$

Outflows can be specified at any depth over the water column and they are accounted for by removing water from the layer at the depth defined at the outlet point and computation of the Grashof number:

$$Gr = \frac{N^2 A_i^2}{v^2}$$

Model Suitability & Data Requirements

The model may be suitable for investigations where resolving the horizontal variability is not a requirement of the study.

The model requires the user to supply a hypsographic curve, $A = A(h)$, to describe the storage, elevation, area and volume relationships, meteorological time-series data for surface forcing, and daily time-series of volumetric inflow and outflow rates. Further details of the model setup and file formats are outlined in the GLM Setup section.

A summary of relevant parameters within the model and their default values are given in Table 1 for general lake parameters, and for the snow-ice model specifically in Table 2.

Table 1. Summary of GLM physical parameters with recommended values and references.

Symbol	glm.nml ID	Description	Units	Default	Reference	Comments
Model Structure						
h_{min}	min_layer_thick	Minimum layer thickness	m	0.5	-	Standardised for multi-lake comparison
h_{max}	max_layer_thick	Maximum layer thickness	m	1.5	-	Should be estimated relative to lake depth.
Lake Properties						
K_w	Kw	Extinction coefficient for shortwave radiation	m^{-1}	0.2	Lake specific	Should be measured, e.g. mean of simulation period
Surface Thermodynamics						
C_h	ch	Bulk aerodynamic coefficient for sensible heat transfer	-	0.0014	Fischer et al. 1979	From Hicks' (1972) collation of ocean and lake data; many studies since use similar values.
C_e	ce	Bulk aerodynamic coefficient for latent heat transfer	-	0.0013	Fischer et al. 1979	
C_m	coef_wind_drag	Bulk aerodynamic coefficient for transfer of momentum	-	0.0013	Fischer et al. 1979	
Q	-	Latent heat of evaporation	$J \ kg^{-1}$	2.453×10^6	Standard	Not adjustable in GLM.nml
Q	-	Emissivity of the water surface	-	0.97 0.95	Standard	Water only, no ice Ice or snow
Q	-	Stefan-Boltzmann constant	$W \ m^{-2} \ K^{-4}$	5.67×10^{-8}		Not adjustable in GLM.nml
Mixing Parameters						
C_k	coef_mix_conv	Mixing efficiency - convective overturn	-	0.2	Yeates & Imberger 2003	Selected by Yeates et al (2004) from a range given in Spigel et al. (1986)
C_w	coef_wind_stir	Mixing efficiency - wind stirring	-	0.23	Spigel et al. 1986	From Wu 1973
C_s	coef_mix_shear	Mixing efficiency - shear production	-	0.3	Sherman et al. 1978	Best fit of experiments reviewed
C_t	coef_mix_turb	Mixing efficiency - unsteady turbulence (acceleration)	-	0.51		
K_H	coef_mix_KH	Mixing efficiency - Kelvin-Helmholtz	-	0.3	Sherman et al. 1978	"a good rule of thumb..."



Symbol	glm.nml ID	Description	Units	Default	Reference	Comments
		turbulent billows				
θ_{TKE}	coef_mix_hyp	Mixing efficiency of hypolimnetic turbulence	-	0.5		
Inflows & Outflows						
C_D	strmbd_drag	streambed_drag	-	0.016		
U_{out}	-	Maximum withdrawal velocity	$m s^{-1}$	-		

Table 2. Summary of ice model parameter descriptions, units and typical values.

Symbol	Description	Units	Default value
I_{e1}	Waveband 1, snow ice light extinction	m^{-1}	48.0
I_{e2}	Waveband 2, snow ice light extinction	m^{-1}	20.0
I_{i1}	Waveband 1, blue ice light extinction	m^{-1}	1.5
I_{i2}	Waveband 2, blue ice light extinction	m^{-1}	20.0
I_{s1}	Waveband 1, snow light extinction	m^{-1}	6
I_{s2}	Waveband 2, snow light extinction	m^{-1}	20
D_z	Distance of heat transfer, ice water	m	0.039
r_e	Density, snow ice	$kg m^{-3}$	890
r_i	Density, blue ice	$kg m^{-3}$	917
r_s	Density, snow	$kg m^{-3}$	Variable
c_{pi}	Heat capacity, ice	$kJ kg^{-1} ^\circ C^{-1}$	2.1
c_{pw}	Heat capacity, ice	$kJ kg^{-1} ^\circ C^{-1}$	4.2
K_c	Compaction coefficient	-	Variable
K_e	Thermal conductivity, snow ice	$W m^{-1} ^\circ C^{-1}$	2.0
K_e	Thermal conductivity, blue ice	$W m^{-1} ^\circ C^{-1}$	2.3
K_e	Thermal conductivity, snow	$W m^{-1} ^\circ C^{-1}$	Variable
K_e	Thermal conductivity, sediment	$W m^{-1} ^\circ C^{-1}$	1.2
K_e	Thermal conductivity, water	$W m^{-1} ^\circ C^{-1}$	0.57
L	Latent heat of fusion	$kJ kg^{-1}$	0334

Setup & Operation

Overview

This section gives a description of the structure of a GLM setup is described. GLM requires a configuration files and several time-series input files and integrates with FABM for water quality simulations (Figure 3).

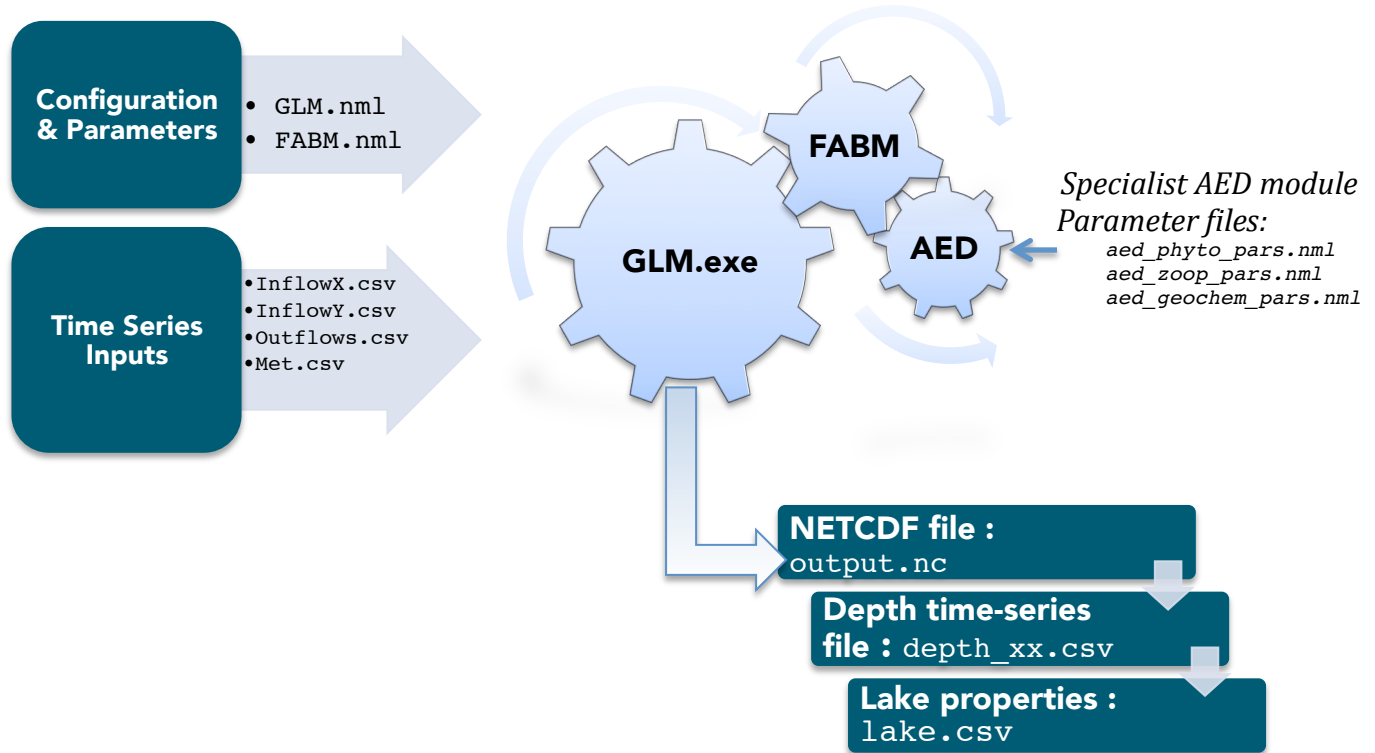


Figure 3: Flow diagram showing the files required for operation of the model.

Input files

Physical model configuration: **glm.nml**

The file glm.nml is the main configuration file for the physical model, and some details related to the FABM coupling. The nml file includes detailed description of the different namelist options for each block; if these value are not present default values will be assumed. It is a namelist file with blocks for:

- &glm_setup: General simulation info
- &wq_setup: Details about the coupling with the water quality model (FABM)
- &time: Time controls
- &morphometry: Lake morphometric information
- &output: Output file details
- &init_profiles: Initial profiles
- &meteorology: Information about surface forcing and meteorology data

- **&inflows:** Information about inflows
- **&outflows:** Information about outflows

Meteorology: **met.csv**

The meteorological conditions are provided as a daily time-series of data with a fixed number of columns, as outlined in Table 3. In future versions sub-daily inputs will be supported. It contains seven compulsory columns, and several optional columns after these depending on the user-defined configuration switches for **snow_sw** and **rain_sw** in the **glm.nml** file.

Table 3: Flow diagram showing the files required for operation of the model.

Met.csv column	Units	Description
(1) TIME	YYYY-MM-DD	Date
(2) SHORTWAVE RADIATION	W/m ²	Daily average shortwave radiation. Note that the daily value is internally distributed to a sub-daily time step by assuming an idealized diurnal cycle.
(3) LONGWAVE RADIATION	W/m ² if lw_type = LW_IN or LW_NET or 0 – 1 if lw_type = LW_CC	Longwave radiation input is either direct incident intensity, net longwave flux, or estimated from cloud cover fraction.
(4) AIR TEMPERATURE	°C	Daily average air temperature 10m above the water surface
(5) RELATIVE HUMIDITY	%	Daily average relative humidity (0-100%) 10m above the water surface.
(6) WIND SPEED	m/s	Daily average wind speed 10m above the water surface
(7) RAINFALL	m/day	Daily rainfall depth
(8) SNOWFALL (optional)	m/day	Daily snowfall depth (optional – include if snow_sw is T)
(9-14) RAINFALL WQ DEPOSITION CONCENTRATIONS (optional)	mg/L	... (optional – include if rain_sw is T)

Inflows: **inflows.csv**

Any number of inflows can be simulated by the model with the configuration and filenames set in the `glm.nml` file. For each inflow there is an associated inflow file of the format outlined in Table 4. At this stage the file only accepts daily data as the inflow calculation is done once a day. It contains four mandatory columns for time, flow, temperature and salinity, and optional columns for water quality constituents.

Table 4: Flow diagram showing the files required for operation of the model.

Inflow.csv column	Units	Description
(1) TIME	YYYY-MM-DD	Date
(2) INFLOW	ML/day	Daily flow rate. Convert from m ³ /s by multiplying by 86.4.
(3) STREAMFLOW TEMPERATURE	°C	Average daily streamflow temperature
(4) STREAMFLOW SALINITY	mg/L	Average daily streamflow salinity
(5 ... $n_{wQ}+4$) STREAMFLOW WATER QUALITY PARAMETER CONCENTRATIONS	mmol/m ³	Average daily streamflow water quality constituent concentrations.

Outflows: **outflows.csv**

Any number of outflow fluxes can be configured and these are set as consecutive columns in the file `outflows.csv` (Table 5). Only daily flow rates are required and water quality variables are not required.

Table 5: Flow diagram showing the files required for operation of the model.

Outflow.csv column	Units	Description
(1) TIME	YYYY-MM-DD	Date
(2 ... $n_{out}+1$) OUTFLOW	ML/day	Daily outflow rates of each outflow

Running the model

The model may be run by navigating to the directory where the `glm.nml` and `fabm.nml` files are and executing the model executable `glm.exe`. The `glm.exe` file can be located in different directory and added to the system path if desired.

Windows users may wish to add the command into a `glm.bat`:

```
..\bin\glm.exe >glm.log
```

which will create a file that can simply be double-clicked from your file browser. The model will output to the NetCDF and/or csv files that can then be plotted.

Note that the Windows pre-compiled model executable is distributed in a 32-bit and 64-bit release; choose an appropriate system.

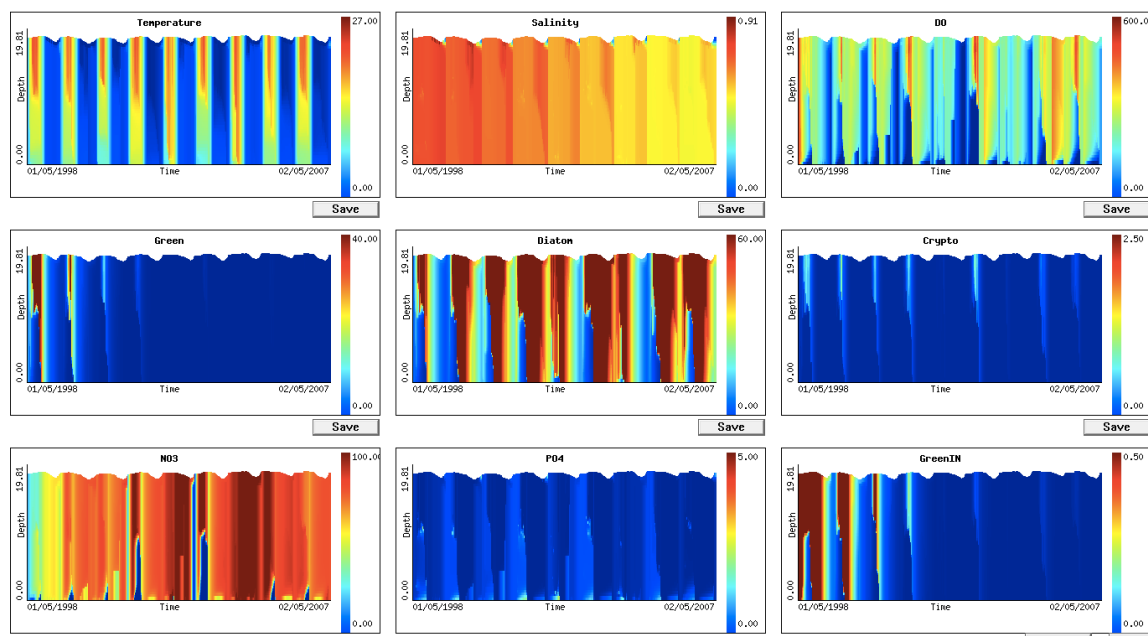
Outputs and post-processing

The model includes several types of outputs, including the NetCDF file, an optional csv time-series file at a certain depth, and an optional live contour plot as the model simulation runs, to enable the modeller to monitor simulation progress.

Live output plotting: `plots.nml`

If the model is run with the optional command line argument "`--xdisp`" then the model simulation will display live plots of output parameters. The number of plots, parameters to plot and the colour bar limits are set in the file `plots.nml`.

```
&plots
nplots      = 4
plot_width  = 400
plot_height = 200
title = 'Temperature','Salinity','DO','Green'
vars  = 'temp','salt','aed_oxygen_oxy','aed_phytoplankton_green'
min_z =  0.0,  0.0,  0.0,  0.0
max_z = 27.0, 0.91, 800.0, 20.0
/
```



Plotting in EXCEL

For simple time-series plots, the user can configure outputs from the model directly to a csv file for a certain depth (defined relative to the bottom, or from the surface), and this information is defined in the `glm.nml &output` section. The columns to plot must also be listed here and are user-definable.

Plotting in R

The GLM output.nc NetCDF file can be read and plotted using the “R” package. A set of tools, rGLM, has been developed in R by Jordan Read and Luke Winslow, and is available from: <https://github.com/GLEON/rGLM>.

Plotting in MATLAB

For more advanced or customised plots, then the user may load the `output.nc` NetCDF file into MATLAB. Recent versions of MATLAB (MATLAB 2011a or after) natively support NetCDF and can load the file directly. An example MATLAB script for plotting is shown below - this can be customised as required.

```
foldername = '../MyGLMSim/';
outname    = '../ MyGLMSim /figures /';
mkdir([outname]);

data       = nldncGLM([foldername,'/output.nc'])

varNames   = names_ncdf([foldername,'output.nc']);
varsToPlot = varNames([20:64]);

for ii = 1:length(varsToPlot)
    newFig  = plotGLM(varsToPlot{ii},data);

    figName = [outname,'/', varsToPlot {ii}, '.png'];
    print(gcf,'-dpng', figName,'-opengl');
    close all
end
```

Model Validation & Parameter Optimisation

There are numerous ways that model users may wish to assess model performance and adjust physical parameters in `glm.nml` to optimise their calibration with observed data. As part of a GLEON (gleon.org) lake modelling working group, a specific workflow for model assessment and parameter estimation has been trialled and is outlined below. The approach a) uses the GLEON “LakeAnalyzer” analysis scripts to assess model comparisons across a range of metrics, and b) combines these assessment scripts with a Markov Chain Monte Carlo (MCMC) method of parameter estimation.

Running the LakeAnalyzer validation

As part of a multi-lake comparison GLM has been compared against numerous different metrics of model performance. These include simple measures like surface or bottom temperature, however it is also possible to compare the model’s performance in capturing higher-order metrics relevant to physical limnology. To calculate these on the model and field data, the LakeAnalyzer routines provided by Read *et al.* (2012). These have been adapted for GLM use and can be called via the run using the `calcGLMModelFit.m` and `plotGLMModelFit.m` scripts. An example output from Lake Kinneret is shown in Figure 4.



Field Files: model_fld_temp.wtr & model.bth

Together the `model_fld_temp.wtr` and the `model.bth` files give observed water temperature data and lake shape details that are compared against the model output. Both files are comma separated text files in the same format as required for running LakeAnalyzer.

The `model_fld_temp.wtr` file is a simple file consisting of time-stamped thermistor chain data. The first row given the date and thermistor chain ID's (Figure 5a). Note the date format must be saved as YYYY-MM-DD, prior to saving as a csv file.

The `model.bth` file is a simple two column file consisting of each thermistors depth, and the area of the bathymetry at that depth (Figure 5b). Save the files as csv.

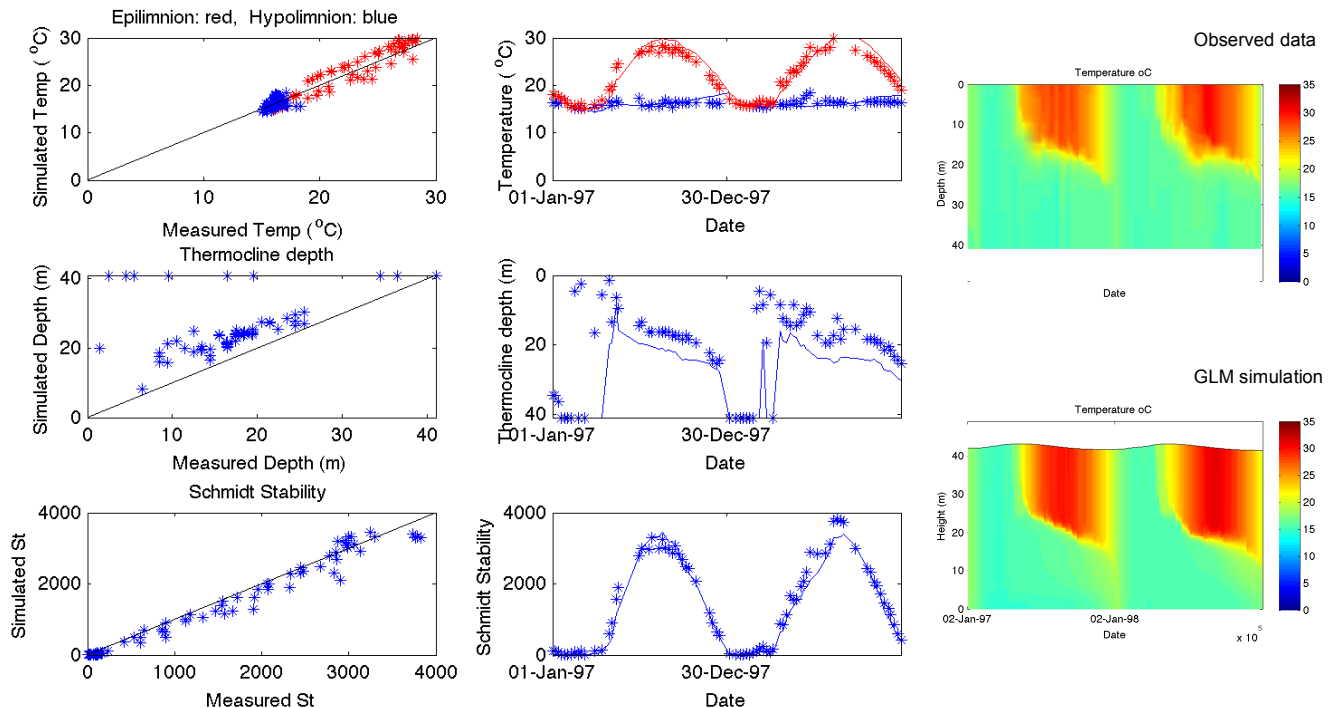


Figure 4: Example output from the GLM model assessment scripts.

Date Time (ISO Format)							Thermistor Chain ID's	
A	B	C	D	E	F	G		
1	DataTime	temp0	temp0.5	temp1.0	temp1.5	temp2.0	temp2.5	
2	1997/01/01 00:00	18.014375	18.0141875	18.014	18.00883333	18.00366667	18.00164583	
3	1997/01/05 00:00	18.014375	18.0141875	18.014	18.00883333	18.00366667	18.00164583	
4	1997/01/14 00:00	17.8175	17.80947222	17.80144444	17.79955556	17.79766667	17.79033333	
5	1997/01/19 00:00	17.36322785	17.36197756	17.36072727	17.34280114	17.324875	17.3104375	
6	1997/01/26 00:00	16.94884375	16.95194568	16.95504762	16.95589881	16.95675	16.95598611	
7	1997/02/02 00:00	16.19581481	16.19803241	16.20025	16.20218056	16.20411111	16.20318056	
8	1997/02/09 00:00	15.3412	15.34665556	15.35211111	15.35186806	15.351625	15.35142361	
9	1997/02/16 00:00	15.95333333	15.92305556	15.89277778	15.867	15.84122222	15.83379861	
10	1997/02/24 00:00	15.16827273	15.16909091	15.16990909	15.16889205	15.167875	15.16438194	
11	1997/03/02 00:00	15.247	16.25240909	16.25781818	16.19484659	16.111875	15.85782639	
12	1997/03/09 00:00	15.22820588	15.20935294	15.1905	15.1785	15.1665	15.1604375	
13	1997/03/16 00:00	15.99888889	15.99727778	15.99566667	15.99138889	15.98711111	15.98499306	
14	1997/03/30 00:00	16.549	16.9179375	16.926875	16.90325	16.879625	16.848	
15	1997/04/13 00:00	19	19	19	18.5	18	18	
16	1997/05/04 00:00	19.8	19.8	19.8	19.8	19.8	19.8	
17	1997/05/13 00:00	23.90209859	23.9003618	23.898625	23.89447917	23.89033333	23.87566667	
18	1997/05/18 00:00	24.57325	24.5649375	24.556625	24.54453472	24.53244444	24.5207222	
19	1997/06/29 00:00	27.4	27.4	27.4	27.35	27.3	27.05	
20	1997/07/06 00:00	27.5	27.5	27.5	27.5	27.5	27.5	
21	1997/07/20 00:00	27.2	27.2	27.2	27.2	27.2	27.2	

Bathymetry Depths	Bathymetry Areas
0	170000
1	167000
4	162000
5	161000
6	160000
7	158000
8	157000
9	155000
10	153000
11	151000
12	150000
13	148000
14	146000
15	143000
16	139000
17	136000
18	132000
19	128000
20	123000
21	118000
22	113000
23	107000
24	102000
25	96400
26	909575

Each Thermistor in the wtr must be represented by a depth

Figure 5: Outline of the required field data files to run the model validation for
a) `model_fld_temp.wtr` and b) `model.bth`.



Running the MCMC parameter estimation

As part of the modelling process, users may desire to adjust the GLM physical parameters to get the best fit with available field data. GLM may be run with a Markov Chain Monte Carlo (MCMC) routine that can be used to provide improved parameter estimates. On the GLM website we provide a version of GLM that works with the MCMC code provided by Haario *et al.* (2006), though users may wish to develop their own optimisation approach.

The MCMC routines are available as MATLAB scripts that will call `glm.exe` during the run. This is run using the `runMCMC.m` script. We have also prepared a pre-compiled form of the procedure that can run on Windows via the command prompt, independent of MATLAB being installed, by running `runMCMC.exe`. Note that for the pre-compiled version that has been supplied, users must have the MATLAB runtime environment (MCR) installed (<http://www.mathworks.com.au/products/compiler/mcr/>).

To run the model as part of the MCMC routine, users must prepare several extra files and directories. These include files for providing the observed field data (as above) and also files associated with the MCMC routine:

- Field/model.bth
- Field/model_fld_temp.wtr
- InputFiles/glm_init.nml
- InputFiles/mcmc_config.nml

The model will run and output a log of model RMSE and other information about the performance of different parameter combinations. These will be written to files in the `Results/` folder.

MCMC files: `glm_init.nml` & `mcmc_config.nml`

The `InputFiles/glm_init.nml` file is simply a duplicate of the starting simulation GLM nml file. The structure of this file is described in the above sections.

The `InputFiles/mcmc_config.nml` file is a namelist file which specifies certain parameters which governs how the optimisation routine functions. Currently, there are four sections:

- `&config`
- `&dataset`
- `&ssh`
- `¶ms`

The `&config` section contains the following variables:

- `Fld_temp_file` – Path to model_fld_temp.wtr file
- `Varname` – GLM variable name of data within the wtr file (e.g. 'temp')
- `Remote` – Switch for whether routine is run locally (0) or an a server via ssh (1)
- `Nsim_ini` – Number of simulations to run to get base values
- `Nsim_full` – Number of optimisation simulations to run.

The `&dataset` section contains the following variables:

- `Data_Subsets`
- `Model_Fit` – Type of error calculation (e.g., RMSE, Nash-Sutcliffe, R², etc)

The `&ssh` section contains the following variables:

- `Host_Name`
- `Usr_Name`
- `Password`
- `Remote_Dir`
- `Run_GLM`
- `Output_File`
- `Varname`



The `¶ms` section contains the following variables and these are those that are to be included in the parameter optimisation. The values assigned to these variables is the starting parameter vector:

- `coef_mix_conv` – Coefficient related to mixing efficiency of convective overturn.
- `coef_wind_shear` – Coefficient related to mixing efficiency of wind shear events.
- `coef_mix_turb` – Coefficient related to mixing efficiency of unsteady turbulence.
- `coef_mix_kh` – Coefficient related to Kelvin Helmholtz turbulent billows.
- `coef_mix_hyp` – Coefficient related to mixing efficiency of hypolimnetic turbulence
- `ce` – Bulk transfer coefficient for latent heat, C_E .
- `ch` – Bulk transfer coefficient for sensible heat, C_H .
- `coef_wind_drag` – Bulk transfer coefficient for momentum, C_D .

Examples & Support

Downloads & Further Support

To download the model, visit: <http://aed.see.uwa.edu.au/research/models/GLM/>

Support and FAQ's are available at the Aquatic Ecosystem Modelling Network (AEMON) website:

<http://sites.google.com/site/aquaticmodelling/>

For specific development requests, please contact Dr Louise Bruce or A/Prof Matthew Hipsey from the School of Earth and Environment, The University of Western Australia.

louise.bruce@uwa.edu.au
matt.hipsey@uwa.edu.au

Example Applications

Numerous applications are presented online as part of the GLM Multi-Lake Comparison Project (MLCP):

<http://aed.see.uwa.edu.au/research/models/GLM/Pages/projects.html>

Two example setups - "warmlake" and "coldlake" - are also available for download. These simulations demonstrate working setups configured using various simulation options, including ice-cover for coldlake.



References

- Ambrose, R.B. Jr., Wool, T.A., Conolly, J.P., and Scahnz, R.W.. 1988. A Hydrodynamic and Water Quality Model: Model Theory, Users Manual, and Programmers manual: WASP4 Environmental Research Laboratory, US EPA, EPA 600/3-87/039, Athens, GA.
- Arhonditsis, G.B., Adams-Vanharn, B.A., Nielsen, L., Stow, C.A., and Reckhow, K.H., 2006. Evaluation of the current state of mechanistic aquatic biogeochemical modeling: citation analysis and future perspectives. *Environ. Sci. Technol.*, **40**: 6547-6554.
- Arhonditsis, G.B., M.T. Brett. 2004. Evaluation of the current state of mechanistic aquatic biogeochemical modeling. *Marine Ecology Progress Series*, **271**: 13–26.
- Bruce, L.C., Hipsey, M.R. and Cook, P.M., Quantification of sediment and water processing of nitrogen in a periodically anoxic urban estuary using a 3D hydrodynamic-biogeochemical model. Submitted to *Journal of Soils and Sediments*.
- Bruce LC, Hamilton DP, Imberger J, Gal G, Gophen M, Zohary T, Hambright KD, 2006. A numerical simulation of the role of zooplankton in C, N and P cycling in Lake Kinneret, Israel. *Ecol. Model.* **193**: 412-436.
- Broekhuizen, N., Rickard, G. J., Bruggeman, J. & Meister, A. 2008. An improved and generalized second order, unconditionally positive, mass conserving integration scheme for biochemical systems. *Applied Numerical Mathematics* 58:319–40.
- Bruggeman, J. 2011. D2.14 Users guide and report for models in the MEECE library – Framework for Aquatic Biogeochemical Models (FABM). Report for the EC FP7 MEECE project 212085. 57pp.
- Burchard H et al. 2005. Application of modified Patankar schemes to stiff biogeochemical models, *Ocean Dyn.*, **55**: 326-37
- Burchard, H., Bolding, K., Kuhn, W., Meister, A., Neumann, T. & Umlauf, L. 2006. Description of a flexible and extendable physical-biogeochemical model system for the water column. *Journal of Marine Systems* 61: 180-211.
- Chao, X., Jia, Y., Shields, F.D., Wang, S.S.Y., and Cooper, C.M., 2010. Three-dimensional numerical simulation of water quality and sediment-associated processes with application to a Mississippi Delta lake. *Journal of Environmental Management* **91**: 1456 – 1466.
- Coles, J.F. and R.C. Jones. 2000. Effect of temperature on photosynthesis-light response and growth of four phytoplankton species isolated from a tidal freshwater river. *J. Phycology*, **36**: 7-16.
- Droop, M.R. 1974. The nutrient status of algal cells in continuous culture. *J. Mar. Biol. Assoc. UK*, **54**: 825–855.
- Fasham, M.J.R., Ducklow, H.W. & McKelvie, S.M., 1990. A nitrogen-based model of plankton dynamics in the oceanic mixed layer. *J Mar Res* 48: 591-639
- Gal, G., Hipsey, M.R., Paparov, A., Makler, V. and Zohary, T., 2009. Implementation of ecological modeling as an effective management and investigation tool: Lake Kinneret as a case study. *Ecol. Model.*, **220**: 1697-1718.
- Griffin, S.L., Herzfeld, M., Hamilton, D.P., 2001. Modelling the impact of zooplankton grazing on phytoplankton biomass during a dinoflagellate bloom in the Swan River Estuary, Western Australia. *Ecological Engineering*, **16**: 373-394.
- Haario, H., Laine, M., Mira, A. and Saksman, E., 2006. DRAM: Efficient adaptive MCMC, *Statistics and Computing* **16**, pp. 339-354.
- Hamilton, D.P. & Schladow, S.G. 1997. Water quality in lakes and reservoirs. Part I Model description. *Ecol. Model.* **96**: 91–110. Hipsey, M.R., Salmon, S.U., Aldridge, K.T. and Brookes, J.D., 2010. Impact of hydro-climatological change and flow regulation on physical and biogeochemical dynamics of the Lower River Murray, Australia. *8th International Symposium on Ecohydraulics (ISE2010)*, September, 2010, Korea.
- Jellison, R. & Melack, J.M. 1993. Meromixis and vertical diffusivities in hypersaline Mono Lake, California. *Limnol. Oceanogr.* **38**: 1008–1019.
- Kilminster et al., 2011. Unpublished data.
- Kromkamp, J. & Walsby, A.E. 1990. A computer model of buoyancy and vertical migration in cyanobacteria. *J. Plankton Res.* **12**: 191–183.

- Kruger, G.H.J. and J.N. Eloff. 1977. The influence of light intensity on the growth of different *Microcystis* isolates. *J. Limnol. Soc. Sth Africa.* **3**: 21-25.
- Imberger, J. and J.C. Patterson. 1981. A dynamic reservoir simulation model-DYRESM:5. In "Transport Models for Inland and Coastal Waters." H.B. Fisher(ed). Academic Press, New York. : 310-361.
- Mooij, W.M., Trolle, D., Jeppesen, E., Arhonditsis, G., Belolipetsky, P.V., Chitamwebwa, D.B.R., Degermendzhy, A.G., DeAngelis, D.L., De Senerpont Domis, L.N., Downing, A.S., Elliott, A.E., Fragoso Jr, C.R., Gaedke, U., Genova, S.N., Gulati, R.D., Håkanson, L., Hamilton, D.P., Hipsey, M.R., Hoen, J., Hülsmann, S., Los, F.J., Makler-Pick, V., Petzoldt, T., Prokopkin, I.G., Rinke, K., Schep, S.A., Tominaga, K., Van Dam, A.A., Van Nes, E.H., Wells, S.A., Janse, J.H., 2010. Challenges and opportunities for integrating lake ecosystem modelling approaches, *Aquatic Ecology*, **44**: 633–667.
- Petrone K.C. Richards, J.S. and Grierson, P.F., 2009. Bioavailability and composition of dissolved organic carbon and nitrogen in a near coastal catchment of south-western Australia. *Biogeochemistry*, **92**: 27-40.
- Read, J. S., D. P. Hamilton, I. D. Jones, K. Muraoka, L. A. Winslow, R. Kroiss, C. H. Wu, and E. Gaiser (2011), Derivation of lake mixing and stratification indices from high-resolution lake buoy data, *Environ. Model. Software* **26**: 1325–1336.
- Rhee, G.Y. & Gotham, E.J. 1981 The effect of environmental factors on phytoplankton growth: temperature and the interactions of temperature with nutrient limitation. *Limnol. Oceanogr.* **26**, pp. 635–648.
- Riley, J.P. & Skirrow, G.. 1974. Chemical Oceanography Academic Press, London.
- Rogers CK, Lawrence GA, Hamblin PF, 1995. Observations and numerical simulation of a shallow ice-covered midlatitude lake. *Limnol. Oceanogr.* **40**: 374-385.Romero, J.R., Antenucci, J.P., & Imberger, J. 2004. One- and Three-Dimensional biogeochemical Simulations of Two Differing Reservoirs. *Ecol. Model.*..
- Robarts, R.D. and T. Zohary. 1987. Temperature effects on photosynthetic capacity, respiration and growth rates of bloom forming cyanobacteria. *N.Z. J Mar. Freshwater Res.* **21**: 391-399.
- Schladow, S.G. & Hamilton, D.P. 1997 Water quality in lakes and reservoirs. Part II Model calibration, sensitivity analysis and application. *Ecol. Model.* **96**: 111–123.
- Sherman, F.S., Imberger, J., and Corcos, G.M. 1978. Turbulence and mixing in stably stratified waters. *Ann. Rev. Fluid Mech.* **10**, 267-288.
- Smith, C.S., Haese, R.R. and Evans, S. 2010. Oxygen demand and nutrient release from sediments in the upper Swan River estuary. *Geoscience Australia Record*, 2010/28. Commonwealth Government, Canberra.
- Smith, C.S., Murray, E.J., Hepplewhite, C. and Haese, R.R. (2007). Sediment water interactions in the Swan River estuary: Findings and management implications from benthic nutrient flux surveys, 2000-2006. *Geoscience Australia Record* 2007/13.
- Spillman, C.M., Hamilton, D.P., Hipsey, M.R. and Imberger, J., 2008. A spatially resolved model of seasonal variations in phytoplankton and clam (*Tapes philippinarum*) biomass in Barbamarco Lagoon, Italy, *Estuarine, Coastal and Shelf Science*, **79**: 187-203.
- Spillman, C.M., Imberger, J., Hamilton, D.P., Hipsey, M.R. and Romero, J.R., 2007. Modelling the effects of Po River discharge, internal nutrient cycling and hydrodynamics on biogeochemistry of the Northern Adriatic Sea. *Journal of Marine Systems*, **68**: 127-200.
- Talling, J. F. 1957. The phytoplankton population as a compound photosynthetic system. *New Phytol.* **56**: 133-149
- Trolle, D., Hamilton, D.P., Hipsey, M.R., Bolding, K., Bruggeman, J., Mooij, W. M., Janse, J. H., Nielsen, A., Jeppesen, E., Elliott, J. E., Makler-Pick, V., Petzoldt, T., Rinke, K., Flindt, M. R., Arhonditsis, G.B., Gal, G., Bjerring, R., Tominaga, K., Hoen, J., Downing, A. S., Marques, D. M., Fragoso Jr, C. R., Søndergaard, M. and Hanson, P.C. 2012. A community-based framework for aquatic ecosystem models. *Hydrobiologia*, **683**(1): 25-34.
- Wanninkhof, R.. 1992. Relationship between windspeed and gas exchange over the ocean. *J. Geophys. Res. (Oceans)* **97**(C5): 7373–7382.
- Webb, W.L., Newton, M., & Starr, D. 1974. Carbon dioxide exchange of *Alnus rubra*: a mathematical model. *Oecologia* **17**: 281–291.

Yeates, P.S. and Imberger, J. 2004. Pseudo two-dimensional simulations of internal and boundary fluxes in stratified lakes and reservoirs. *Int. J. Riv. Basin Res.* **1**: 1-23.